Aerosol Daytime Variations over North and South America Derived from Multiyear AERONET Measurements

Yan Zhang[1,2], Hongbin Yu[3,2], Tom F. Eck[1,4], Alexander Smirnov[5,4], Mian Chin[6], Lorraine A. Remer[2], Huisheng Bian[7,2], Qian Tan[1,6], Robert Levy[8,2], Brent N. Holben[4], Sabino piazzolla[9]

1. Universities Space Research Association, Columbia, Maryland
2. Climate and Radiation Laboratory, NASA Goddard Space Flight Center, Greenbelt, Maryland
3. Earth System Science Interdisciplinary Center, University of Maryland, College Park, Maryland
4. Hydrospheric and Biospheric Sciences Laboratory, NASA Goddard Space Flight Center, Greenbelt, Maryland
5. Sigma Space Corporation, Lanham, Maryland
6. Atmospheric Chemistry and Dynamics Laboratory, NASA Goddard Space Flight Center, Greenbelt, Maryland
7. Joint Center for Earth Systems Technology, University of Maryland Baltimore County, Baltimore, Maryland
8. Science System Application Inc., Lanham, Maryland
9. NASA Jet Propulsion Laboratory, Pasadena, CA

Correspondence:

Dr. Yan Zhang
NASA GSFC Code 613
Greenbelt, Maryland 20771
Yan.Zhang@nasa.gov
301-614-6153

Abstract: This study analyzes the daytime variation of aerosol with seasonal distinction by using multi-year measurements from 54 of the Aerosol Robotic Network (AERONET) sites over North America, South America, and islands in surrounding oceans. The analysis shows a wide range of daily variability of aerosol optical depth (AOD) and Angstrom exponent depending on location and season. Possible reasons for daytime variations are given. The largest AOD daytime variation range at 440 nm, up to 75%, occurs in Mexico City, with maximum AOD in the afternoon. Large AOD daily variations are also observed in the polluted mid-Atlantic U.S. and U.S. West Coast with maximum AOD occurring in the afternoon in the mid-Atlantic U.S., but in the morning in the West Coast. In South American sites during the biomass burning season (August to October), maximum AOD generally occurs in the afternoon. But the daytime variation becomes smaller when sites are influenced more by long-range transported smoke than by local burning. Islands show minimum AOD in the morning and maximum AOD in the afternoon. The diverse patterns of aerosol daytime variation suggest that geostationary satellite measurements would be invaluable for characterizing aerosol temporal variations on regional and continental scales. In particular, simultaneous measurements of aerosols and aerosol precursors from a geostationary satellite would greatly aid in understanding the evolution of aerosol as determined by emissions, chemical transformations, and transport processes.

1. Introduction

Tropospheric aerosols have large spatial and temporal variations that are controlled by changing emissions from diverse origins, by meteorological processes on various scales, by chemical evolution, and by removal processes. The characteristic time scale of variation of aerosol optical depth is about 3 hours in remote regions, but can be less than 1 hour near the emission sources [Anderson et al., 2003]. High spatial and temporal resolution measurements of aerosol are essential for improving particulate matter (PM) air quality forecasts. Aerosol daytime variations, in combination with changing geometry of Sun and surface reflectance, could lead to large daytime variations of aerosol radiative forcing [Yu et al., 2004]. Such variations of aerosol forcing need to be adequately represented in a model in order to realistically assess atmospheric responses to the radiative forcing, such as the atmosphere-surface interactions and the evolution of the atmospheric boundary layer [Yu et al., 2002]. Aerosols interact with clouds on the cloud lifetime scales which are significantly less than an hour. Finally, aerosol variations need to be taken into account when comparing different observations or integrating observations and models [Anderson et al., 2003; 2005]. For all these reasons, high temporal resolution aerosol measurements are needed and the day time variations of aerosol loading need to be quantified.

Surface networks and aircraft missions have made progress towards quantifying aerosol daytime variations [e.g., Kaufman et al, 2000; Smirnov et al., 2002; Delene and Ogren, 2002; Anderson et al., 2003; Pandithurai et al., 2007; Michalsky et al., 2010]. However, such studies are limited in spatial extent and/or longevity. Although polar orbiting satellites can survey the entire globe with high spatial resolution, they can only sample a particular location once a day. The daytime variations of aerosols on a large spatial scale can however be measured from geostationary earth orbit [e.g., Wang et al., 2004; Prados et al., 2007]. The major advantage of

79 a geostationary measurement is its regional and continental coverage with high time and space
80 resolution, which surface and aircraft measurements can never achieve. Current geostationary
81 satellites sensors, such as The Geostationary Operational Environmental Satellites (GOES),
82 were not designed to retrieve aerosol information with the coarse spatial resolution and limited
83 wavelength band, such that the aerosol products from GOES have never reached the same
84 level of accuracy and quality as the aerosol products from the EOS-era polar orbiting missions.
85 The U.S. National Research Council [NRC, 2007] has recommended the Geostationary Coastal
86 and Air Pollution Events (GEO-CAPE) mission for the coming decade to advance science and
87 meet societal needs in relation to atmospheric-pollution chemistry, climate forcing, and coastal
88 ecosystems. This mission offers an opportunity to design a geostationary satellite
89 measurement of daytime variations aerosols and precursor gases with improved accuracy to
90 advance the understanding of aerosol processes and aerosol effects on climate and air quality.

91 As part of a NASA-led effort to define the science requirements for the aerosol
92 component of the GEO-CAPE mission [Fishman et al., Progress Report on NASA's GEO-CAPE
93 Mission, submitted to *Bull. Amer. Meteor. Soc.*, 2011], this study analyzes the daytime variation
94 of aerosol with seasonal distinction by using multi-year measurements from 54 of the Aerosol
95 Robotic Network (AERONET) sites over North America, South America, and islands of the
96 surrounding oceans (i.e., within the planned geographical coverage of GEO-CAPE). Both
97 aerosol loading and size/type, as characterized respectively by aerosol optical depth (AOD) and
98 Angstrom exponent (AE), are examined. The rest of paper is organized as follows. We give an
99 overview of major factors contributing to aerosol daytime variations in Section 2 to facilitate later
100 discussions. Section 3 describes the AERONET datasets and method of calculating daytime
101 variations. Section 4 presents the spatial patterns of aerosol daytime variation in the study
102 domain and then discusses in more detail the aerosol daytime variation in several

representative regions or sites. Major conclusions and implications for the GEO-CAPE mission are summarized in Section 5.

2. Factors contributing to aerosol daytime variations

Daytime variation of aerosol optical depth (AOD) and Angstrom exponent (AE) can be attributed to such factors as emissions, meteorological conditions, photochemical activities, and relative humidity (RH), among others. In what follows, we briefly describe several of these major factors. In reality, several factors usually work together to determine the aerosol daytime variation.

Emission: Daytime variations of particle emissions directly control variations of AOD and probably AE, particularly in source regions. For example, biomass burning in South America is generally more active in the afternoon than in the morning [Prins et al., 1998], suggesting that AOD in smoke source regions is also higher in the afternoon. Over urban areas, aerosol and its precursor emissions are larger during rush hours than non-rush hours, contributing to the AOD and AE diurnal variation.

Meteorology: Meteorological conditions, in particular those associated with meso-scale circulations, control the transport, evolution, and removal of aerosols on a daily time scale. For example, the land-sea breeze and mountain-valley circulations resulting respectively from differential heating between land and sea, and between mountain and valley, can play an important role in diluting or accumulating aerosols. The daytime sea breeze would bring maritime air into the continental boundary layer, which may lower the aerosol loading and increase the size of aerosol. The night time land breeze would bring continental air from inland to coastal area, possibly resulting in accumulation of aerosols in the coastal area. Similarly, the daytime upslope flow would bring polluted air from foothill to relatively pristine hilltops, and result in an increase of AOD over the day and a peak in the afternoon on the hilltop. Rain-out and

128 wash-out are major scavenging mechanisms for aerosols. Therefore, the diurnal variation of
129 clouds and precipitation would regulate diurnal variation of aerosols.

130 *Photochemistry*: Secondary aerosol, such as sulfate, nitrate, and some organic aerosols
131 are produced from precursor gases through photochemical processes. Such photochemical
132 production rates for aerosols are determined by diurnal varying photodissociation frequencies
133 that increase with increasing solar radiation and sometimes temperature. Aqueous chemistry is
134 also one of the major chemical pathways for the formation of aerosols such as sulfate.

135 *Hygroscopic growth*: Hydrophilic aerosols, like sulfate, sea salt, nitrate, and some types
136 of carbonaceous aerosol, can grow when the ambient relative humidity (RH) increases [Seinfeld
137 and Pandis, 1998, Bian et al, 2009]. An increase of RH increases the particle size and hence
138 the cross-section of particle interacting with solar radiation, leading to an increase of AOD and
139 decrease of AE. This process is highly non-linear, with the rate of particle growth much higher
140 at high RH than at low RH. Dust, black carbon, and some organic carbon aerosols are, by
141 contrast, largely hydrophobic and their size change little with variation of RH.

142

143 **3. AERONET data and analysis method**

144 AERONET is a federated international ground-based global network established for
145 characterizing aerosol optical properties and validating aerosol satellite retrievals [Holben et al.,
146 1998]. The network started in 1993 and has since been expanded to more than 500 sites
147 globally over nearly two decades. Typically most Cimel Sun-sky radiometers deployed by
148 AERONET measure the direct solar irradiances in wavelength channels 340, 380, 440, 500, 675,
149 870, 940, and 1020 nm (some have an additional channel at 1640 nm) with a nominal sampling
150 frequency of 15 minutes (higher frequency in early morning and late afternoon in order to
151 attempt Langley calibrations). Among the direct-sun channel, the 940 nm one is designed to
152 estimate total precipitable water content and the remaining seven are used to retrieve AOD. An

153 automatized and computerized cloud-screening algorithm [Smirnov et al., 2000] is applied after
154 AOD is calculated. The typical uncertainty in AOD for Level 2 AERONET data is ±0.01 to ±0.02,
155 with the larger errors appearing in ultraviolet bands [Eck et al., 1999]. The wavelength (λ)
156 dependence of AOD, is characterized by Angstrom Exponent (AE) with the classical equation
157 $AOD(\lambda) \sim \lambda^{-AE}$ (Angstrom, 1929). AE can be used as a proxy for aerosol size, with a value
158 greater than 1 indicating fine-mode (sub-micron radius) pollution and biomass burning aerosols
159 and a value less than ~0.6 indicating coarse-mode (super-micron radius) dust and sea-salt
160 aerosols. In this study, we use only Version 2 Level 2 AERONET data, and derive AE from a
161 linear fitting of versus , using measurements at the 4 CIMEL wavelengths in the range
162 of 440-870 nm, following Eck et al. [1999].

163 A total of 54 AERONET sites, mainly located in both South America and North America,
164 and on islands in the surrounding oceans, were selected for this study. All these sites have at
165 least two years of measurements available after 1997 (note that interference filter type was
166 changed in 1997, with significant improvement in filter transmittance stability). Measurements
167 prior to 1997 are excluded to retain only measurements with the highest quality calibration. We
168 consider only the data that fall within the ranges of $0.01 < AOD < 5$ and $0 < AE < 3$ to eliminate
169 unrealistic measurements. 92% of the data fall within these ranges for all sites. Given that the
170 sample frequency and total number of measurements differ from site to site, all individual
171 observations in a day are expressed as the departure (percentage) from the daily mean to avoid
172 sampling number issues [Smirnov et al., 2002]. The calculation of diurnal average departure
173 (percentage) for each season of AOD and AE for each AERONET site is as follows: 1) compute
174 hourly mean AOD and AE by averaging all available instantaneous measurements within one
175 hour, for example, between 10:30 a.m. and 11:30 a.m. local time for each day; 2) calculate the
176 daily mean by averaging all available hourly means, excluding days with less than five hourly
177 means; 3) calculate percentage departures of individual hourly observations from the daily

178 mean; 4) derive seasonal mean of hourly departure (percentage) by aggregating all hourly
179 departures from the daily mean within an hour in a given season. We divide the data into the
180 usual four seasons, namely Dec-Feb (DJF), Mar-May (MAM), Jun-Aug (JJA), and Sep-Nov
181 (SON), except as otherwise specified. Daytime variation range (referred to as DVR, in
182 percentage) is defined as the difference between the maximum and minimum hourly departure
183 (in percentage) in a season. DVR combined with seasonal mean AOD and AE can be used to
184 approximately estimate the absolute range of change over a day.

185 **4. Results**

186 **4.1 Spatial patterns of aerosol daytime variations**

187 Figures 1 and 2 give an overview of daytime variations of AOD and AE, respectively, in
188 all 54 AERONET sites on a seasonal basis. In these figures, seasonal means of AOD and AE
189 are represented by different colors; DVRs by the size of triangle, and the occurring time of peak
190 AOD or AE by the direction of triangle (see figure legends for details). These figures show a
191 wide range of aerosol daytime variations, in terms of both DVR and occurring time of maximum
192 value, depending on location and season. Mexico City has the largest AOD and the highest
193 AOD daytime variations throughout the year, with DVR of 30-50% or higher. The maximum
194 AOD occurs in the morning in summer and in the afternoon in other seasons.

195 In the eastern part of the U.S. where industrial pollution dominates, AOD is generally
196 highest in summer and lowest in winter. The high summertime AOD is associated with high
197 relative humidity, active photochemistry, and stagnant atmospheric circulations [Husar et al.,
198 1981, Bian et al., 2010]. The DVR for AOD is generally larger than 10%, with the highest value
199 about 30%. Maximum AOD for each season occurs in the afternoon. The daytime variations for
200 AE in the eastern US are generally small (less than 10%), particularly in summer (~ 5%).

201 In the western part of the U.S., AOD DVRs are generally comparable to those in the
202 eastern part of the U.S. in summer but smaller in other seasons. Given that the mean AOD is

smaller in the west than in the east, the absolute daytime variation of AOD in the west is smaller than that in the east. Also the maximum AOD generally occurs in the morning in the west, which is opposite to that in the east. On the other hand, DVRs of AE in the west are significantly larger than that in the east in the summer and winter, suggesting that particle size or aerosol type in the west undergoes larger changes in the course of a day. However uncertainties in computed AE are much larger at low AOD (given the AOD measurement uncertainty of ~0.01), therefore the larger DVR of AE in the west can be due at least in part to greater AOD uncertainties.

Over South America, in the wet season (DJF and MAM), coarse-mode biogenic aerosols from forests are a major component and some sites are also influenced by the long-range transport of Saharan dust and African smoke [Ansmann et al., 2009]. As such, AE in the wet season is relatively small, with a range of 0.8-1.2 for most sites but less than 0.8 in some sites. In the wet-to-dry transition and dry season (JJA and SON), biomass burning smoke dominates over biogenic aerosols and AE is generally greater than 1.5.

In island sites over the tropical Pacific Ocean and Atlantic Ocean where aerosol is dominated by marine aerosol with little influence from continental sources, both AOD and AE are generally smaller than that over the continents. However the relative daytime variations of marine aerosol are generally large. For AOD, DVR generally falls into a range of 10~30% for all seasons, which however does not necessarily mean large absolute change of AOD because of small AOD values. For AE, the DVR is generally higher than 20%, with the highest value of more than 40% in Lanai in summer. While small AOD values over the ocean would have introduced large uncertainties in AE and its variations, the observed large daytime variations of AE are indeed consistent with some physical explanations to be discussed later.

In the following sections, we examine in more detail the daytime variations of AOD and AE in several regions/sites representative of urban and industrial pollution, biomass burning smoke, marine aerosol, and free-atmosphere aerosol.

229

230 4.2 **Urban and industrial pollution aerosols**

231 *Mid-Atlantic U.S.:* Several urban/suburban sites are located in the mid-Atlantic U.S.,
232 including the Goddard Space Flight Center (GSFC), the Maryland Science Center in Baltimore
233 (MDSC), City College of New York City (CCNY), the ocean platform of CERES Ocean
234 Validation Experiment (COVE, off the coast of southern Virginia), Wallops Island (Virginia), and
235 the Smithsonian Environmental Research Center (SERC, on the shore of the Chesapeake Bay
236 in Maryland). As shown in Figure 3, these sites have comparable aerosol loading with high
237 AOD (440 nm) of 0.44-0.50 in summer and low AOD of about 0.1 in winter. The daytime
238 variation of AOD in spring and fall shows a pattern similar to but of lesser magnitude than that in
239 summer. In summer, all the sites show similar patterns of daytime AOD variation: a slight
240 increase of AOD in the morning but a great increase of AOD in the afternoon. The DVR is
241 about 20%, corresponding to AOD change of ~0.09 for GSFC, MDSC, CCNY, and SERC. For
242 two coastal sites, COVE and Wallops, the DVR is less than 10%. Our results based on 12
243 years of observations from GSFC are consistent with that from an earlier study based on 1993-
244 2001 measurements [Smirnov et al., 2002]. These variations are likely associated with the
245 photochemical production and hygroscopic growth as discussed in Section 2. Because particles
246 in the northeastern U.S. are mainly secondary sulfate aerosols [Bian et al., 2010] that are
247 formed via photochemical and aqueous phase reactions [Malm, 1992], the increase of AOD
248 over the daytime can be associated with photochemical processes, and at times also cloud
249 processing. It is observed that the photochemical processes generally start in the early morning
250 and persist about a half day [Sun et al., 2011].

251 Given that sulfate is highly hygroscopic, a change of ambient RH over the day would
252 contribute to the diurnal variation of AOD. The RH change over the day depends on altitude and
253 location, as shown in Figure 4 for the six sites based on GEOS-4 assimilated meteorology in
254 2007 (similar daytime variations occur in 2006 and are not shown here). Over Wallops, RH

255 decreases from morning to afternoon at all altitudes and thus the AOD increase during the day
256 cannot be explained by the hydroscopic growth. For the other five sites, the decrease of RH
257 from morning to afternoon within the boundary layer would result in a decrease of AOD from
258 morning to afternoon, which is however compensated by the increase of aerosol extinction due
259 to the increase of RH near the top of the boundary layer. Although the RH increase near the top
260 of the boundary layer is efficient in increasing the aerosol extinction because of the relatively
261 high RH value, a majority of aerosols in the region stays within the boundary layer [e.g., Yu et
262 al., 2010]. It is thus expected that the overall effect of RH change on AOD daytime variation
263 may be relatively small. In winter, AOD is small and daytime variation range of AOD is <10% for
264 most of those sites. High AOD in the morning and late afternoon in winter is consistent with the
265 diurnal emission from local traffic. Unlike AOD, aerosol AE has a small daytime variation range
266 of less than 10% (0.16) at all sites (not shown).

267 *Southwestern U.S.:* Differing from the northeastern U.S., the mean AOD at several
268 California sites (Fresno, La Jolla, Monterey, and San Nicolas) show relatively small seasonal
269 variations. AOD daytime variation in summer is also opposite to that in the northeastern US, as
270 shown in Figure 5a. AOD has its maximum in the morning and then decreases significantly until
271 reaching a minimum in late afternoon, with DVR ranging from 20% to 38%. Correspondingly the
272 absolute daytime change of AOD is 0.02~0.06, which is smaller than that at the northeastern
273 sites, due to lower AOD not smaller DVR. This is qualitatively consistent with in situ
274 measurements of aerosol concentrations in the region [Fine et al., 2004]. Similar daytime
275 variation patterns are found in fall but with smaller magnitude. In winter and spring, no
276 significant daytime variation is found (not shown). Such aerosol daytime variation is strongly
277 controlled by the meso-scale circulations associated with unique topography in the region. For
278 the three coastal sites in the Los Angeles basin and nearby, namely La Jolla, Monterey, and
279 San Nicolas (an island that is about 100 km offshore), the land-sea breeze circulations

280 interacting with mountain ranges to the east of the basin control the evolution of aerosol [Cass
281 and Shair, 1984; Wakimoto and McElroy, 1986; Lu and Turco, 1994, 1995]. At night the land
282 breeze blowing towards the ocean assisted by mountain katabatic winds takes air pollutants
283 from inland regions to the shore and offshore islands, resulting in an accumulation of pollutants
284 in the coastal region [Cass and Shair, 1984]. This nighttime pollution accumulation, in
285 combination with morning traffic, leads to a morning maximum AOD. With the development of
286 the sea breeze during the day, relatively clean air from the ocean dilutes aerosol and lowers the
287 AOD. Located further inland, Fresno is the second largest metro area in the Central Valley of
288 California. There, AOD diurnal variation is closely related to the surface wind field pattern,
289 especially in summer [Green et al., 1992]. Nighttime stable atmospheric stratification prevents
290 the exit of air from the valley, causing accumulation of pollutants in the site. This in combination
291 with morning traffic leads to a morning maximum AOD. During the day, a valley wind system
292 develops with up-valley flow that ventilates pollutants out of the valley and reduces AOD. In
293 addition, changes in relative humidity may also contribute to the aerosol daytime variation.
294 Daytime variation of AE could be 20-30% at La Jolla for both summer and fall, as shown in
295 Figure 5c and 5d, respectively. The noontime peak AE may be associated with the decreasing
296 relative humidity (decreasing particle size) and increasing photochemical activities (generating
297 fine particles) from morning to noon and the dilution of small pollution particles with large marine
298 particles as sea breeze brings in marine air in the afternoon.

299 *Mexico City*: Aerosol daytime variations in Mexico City, one of the most polluted
300 megacities in the world [Molina et al., 2007], are somewhat different from those in the northeast
301 and western U.S. As shown in Figure 6, seasonal mean AOD ranges from 0.38 in DJF to 0.51
302 in MAM; and seasonal mean AE is about 1.5 in all seasons, indicating the predominance of
303 pollution aerosols throughout the year. Generally AOD increases from early morning, reaches
304 maximum at noon or in early afternoon, and then more or less levels off. The daytime variation

range of AOD is as large as 75% (corresponding to AOD change of 0.28) in DJF and 30-50% (corresponding to AOD change of 0.12-0.20) in other seasons, which is much stronger than that over the urban areas of the northeastern U.S. The daytime variation of AE is 10-15% with a peak in the late morning for all seasons, which is also larger than at GSFC.

The daytime changes of AOD and AE in Mexico City are likely a combined effect of emission, photochemistry, and meteorological conditions associated with the complex topography. Mexico City is located within a basin confined on the east, south, and west sides by mountain ridges of about 1000 m in height with a broad opening to the north and the gap in the mountains at the southeast end of the basin. Local industrial and automobile emissions are two major sources of aerosol [Molina et al., 2007]. The precursor emissions of secondary organic aerosol (SOA) are higher in the morning than in the afternoon. SOA is efficiently formed shortly after sunrise [Molina et al., 2007]. In the morning, the city's unique topography and frequent atmospheric inversions trap the pollutants within the basin, likely leading to rapid increase of AOD throughout the morning [Whiteman et al., 2000, Fast et al., 2007]. In the afternoon, while the photochemical processes continue to produce aerosols, the basin is efficiently vented by terrain-induced winds. For example, the frequently developed strong southeasterly flow due to differential atmospheric heating [Raga et al., 1999, Doran and Zhong, 2000] brings in clean air from outside of the basin through the terrain gap in the southeastern corner and dilutes pollution in the city, resulting in the leveled-off or slight decrease of AOD in the afternoon. Photochemical processes generate new particles, which are small in size, at late morning and noon [Salcedo et al., 2006], yielding a large AE. As the afternoon progresses those small particles are joined by large-size dust, kicked up by local winds, causing the AE to decrease.

4.3 Biomass burning aerosols in South America

In the dry and dry-to-wet transition season (typically from August to October or ASO) of the central and southern Amazon, land clearing and pasture maintenance practices generate a large amount of carbonaceous aerosols [Andreae and Crutzen, 1997; Schafer et al., 2008]. Typically aerosol from biomass burning smoke accounts for ~90% of the fine particles and ~50% of the coarse particles [Martin et al., 2010]. Figure 7 shows daytime variations of AOD for four sites over the Amazon region, including Abracos Hill, Alta Floresta, Cuiaba-Miranda, and Rio Branco. AOD in all these sites show comparable seasonal mean AOD (0.72~0.96). A slight AOD decrease in the early morning and large increase in the afternoon have been observed for both Abracos Hill (about 15%) and Rio Branco (about 22%). On the other hand, in Alta Floresta and Cuiaba-Miranda, AOD generally shows both early morning and late afternoon peaks, with the minimum AOD around noon. The increase of AOD in the afternoon for all the sites is generally consistent with the documented occurrence of peak fire activities in the late morning and middle afternoon [Prins et al., 1998] as a result of higher temperature, lower relative humidity, and stronger winds in the afternoon [Eck et al., 2003, Rissler et al., 2006]. The AOD peaks in the early morning over Alta Floresta and Cuiaba-Miranda may have resulted from the long-range transport of smoke through the night, since both sites are usually influenced by both local biomass burning and long-range transport of aged smoke [Prins, et al., 1998, Reid et al., 1999]. Further analysis for Alta Floresta and CUIABA_MIRANDA as shown in Figure 8 indicates that the AOD daytime variation changes with month. While the AOD daytime variation in September and October is similar to the seasonal average, AOD in August actually increases through the morning and peaks in late afternoon. These different daytime variations in different months are generally consistent with changing locations of biomass burning source regions with month. As discussed in Reid et al. [1999], these two sites are predominantly influenced by local pasture and grass fires in the early burning season but become more influenced by well-aged smoke transported from burning in the forest region in the late burning season (after mid-September).

356

357 **4.4 Marine aerosols**

358 In remote oceans where continental influences are minimal, aerosol is composed of sea
359 salt and organics from sea spray, plus sulfate from DMS oxidations [Lewis and Schwartz, 2004].
360 While sea-salt is dominated by coarse-mode particles, sulfate and organic aerosol are fine-
361 mode. AERONET observations show that marine aerosol is bimodal, with a fine mode at
362 effective radius of 0.11~0.14 um and a coarse mode at 1.8~2.1um [Smirnov et al., 2003].
363 Figure 9 shows AOD and AE variations in Lanai, Hawaii. Lanai, with population of ~3000, is
364 mainly affected by marine aerosol with some influence from local pollution and springtime Asian
365 pollution and dust, although episodic events of high sulfate AOD occur from the emissions of
366 nearby Kilauea and Mauna Loa volcanoes in Hawaii. AOD of 0.11 in spring is larger than 0.07-
367 0.08 in other seasons, which is likely associated with springtime Asian transport [Eck et al.,
368 2005]. The AOD daytime variation is similar in all seasons, with an early morning minimum and
369 a late afternoon maximum. The daytime variation range is about 25%, corresponding to an
370 AOD change of about 0.02. While 0.02 is comparable to the uncertainty of AERONET AOD
371 measurements, the consistent daytime change shown by multi-year data might be indicative of
372 physical processes. For example, the observed daytime variation may be linked to the
373 alternation of wind direction between day and night. At night the island surface cools faster than
374 surrounding ocean, which generates a wind from island toward ocean that cleans up the island.
375 This may lead to a morning minimum AOD. During the day, the island warms faster than the
376 ocean, resulting in a wind from ocean to island. This wind brings in marine aerosol and
377 precursors (e.g., DMS) to island, which in combination with increasing photochemical activities
378 could lead to a gradual increase of AOD during daytime. As shown in Figure 9, AE shows
379 significant daytime variations with a peak around noon. The DVR for AE is about 10% in DJF
380 and MAM but as much as 30% in JJA and SON. Although the large uncertainty of aerosol AE in
381 such low AOD regime makes the detection of daytime variation difficult, the consistent daytime

382 variation may indicate that active photochemistry produces fine-mode sulfate aerosol and
383 increases the AE around noon. However, aerosols on small islands, i.e., Midway Island and
384 Bermuda, show a very small daytime variation with a very flat curve (figure not shown here).
385 Because these two islands are tiny compare to Lanai, only a few kilometers in width and/or
386 length, aerosol properties on those islands remain close to the open ocean values.
387
388 **4.5 Free-atmosphere aerosol**
389 Table Mountain is located at an elevation of 2200 m in the San Gabriel Mountains,
390 California, above Los Angeles, and it samples mainly free-atmosphere aerosol. As shown in
391 Figure 10, the site has seasonal average AOD below 0.1 throughout the year. In DJF, the
392 number of observations is too small to be used for detecting meaningful aerosol daytime
393 variations. In other seasons, AOD consistently increases during the day and reaches a
394 maximum in early afternoon. The AOD daytime variation range is about 25% in MAM and up to
395 35% in JJA and SON. The increase of AOD during the day is likely associated with the
396 evolution of mountain-valley flows. After sunrise, the differential heating of atmosphere between
397 the slope and nearby valley leads to upslope flows that could ventilate pollution from the Los
398 Angeles basin upward to Table Mountain [Wakimoto and McElroy, 1986; Lu and Turco, 1995].
399
400 **5. Concluding remarks**
401 We have analyzed the daytime variations of aerosol optical depth and Angstrom
402 exponent from 54 AERONET sites over the Americas and a few nearby islands on a seasonal
403 basis. The analysis shows a wide range of AOD and AE daytime variations, depending on
404 location and/or season. Mexico City shows the largest AOD in the afternoon, with a daytime
405 variation range (DVR) at 440 nm of up to 75%. Such daytime changes of AOD are likely a
406 combined effect of emissions and complex meteorology associated with the mountainous
407 topography. In the Mid-Atlantic U.S. several urban and suburban sites show consistently large

DVR of AOD with the afternoon maximum, particularly in summer, which is likely associated with strong afternoon photochemical activities. On the other hand, several sites in the U.S. West coast show relatively large DVR of AOD with the early morning maximum, possibly a combined effect of emission and topography-induced mesoscale circulations (such as land-sea breeze circulations and mountain-valley flows) and emissions. Similarly, the atmospheric boundary layer pollution aerosol can be transported upward by upslope flows associated with mountain-valley differential heating, resulting in an AOD increase throughout the day at high mountain sites. In the central part of the U.S., aerosol daytime variations are generally small. Overall, human-influenced sites show a much larger daytime variation than natural sites.

In Brazil, AOD in the burning season increases over the day with the late afternoon maximum consistent with observed peak biomass burning activities in mid- to late-afternoon. However, in some sites AOD in the late burning season (late August to September) shows small daytime variation or even a morning maximum, which is likely associated with the increasing contribution of long-range transported smoke.

Over islands of the remote Pacific Ocean with minimal influences from local anthropogenic activities and from long-range transport of aerosols from upwind continents, AOD has an early morning minimum and a late afternoon maximum, which is presumably associated with land-sea breeze. Aerosol AE in the islands shows the largest value around noon, which may indicate an increase of fine-mode non-sea salt sulfate due to active photochemistry. For the open ocean, i.e., small islands like Midway and Bermuda, no obvious daytime variation of aerosol have been observed.

In general, our study shows two typical daytime variations for AOD in a majority of AERONET sites: (1) AOD continuously increases during the day, reaching a maximum in the afternoon; (2) AOD peaks in the early morning but continuously decreases during the day. It

appears that observations from polar orbiting satellites, such as Terra and Aqua, can't capture the maximum AOD, but may provide a good estimate of the daily average, although this would be by accident not by design since there are only two samples per day. To adequately capture the daytime variations, geostationary satellites such as the planned GEO-CAPE would need to make at least three successful aerosol retrievals during daytime in order to avoid aliasing. Given the often presence of clouds, satellites would need to be designed to sample at an hourly frequency.

We have discussed some possible causes for the observed aerosol daytime variations based largely on previous studies of aerosol emissions, photochemical activity, and large-scale and mesoscale meteorology. Such discussion is generally qualitative in nature and not all variations are fully understood. To better understand the observed complex daytime variations, both comprehensive datasets and high-resolution chemical transport model simulations are needed. Comprehensive dataset of both aerosol and gaseous precursors at regional and continental scale with high temporal resolution cannot be obtained from low-Earth orbit but only from geostationary satellite missions. The unique capability of GEO-CAPE to simultaneously measure aerosol and its precursors would offer insights into how aerosol sources, chemical transformations, and transport processes determine the evolution of atmospheric aerosols on the hourly time scale.

Acknowledgement: The work was supported by NASA as part of efforts for GEO-CAPE aerosol science definition under Dr. Jay AL-Saadi. We are grateful to Shobha Kondragunta, Robert Chatfield, and Warren Wiscombe for helpful discussions and insightful comments.

454
455 **References**

456 Andreae, M. O., and P. J. Crutzen (1997), Atmospheric aerosols: Biogeochemical sources and role in atmospheric
457 chemistry, *Science*, **276**, 1052–1058, DOI: 10.1126/science.276.5315.1052

458 Anderson, T., R. J. Charlson, D. M. Winker, J. A. Ogren, and K. Holmen (2003), Mesoscale variations of
459 tropospheric aerosols, *J. Atmos. Sci.*, **60**, 119-136, 2003. doi: 10.1175/1520-0469

460 Anderson, T., R. J. Charlson, N. Bellouin, O. Boucher, M. Chin, S. A. Christopher, J. Haywood, Y. Kaufman, S.
461 Kinne, J. A. Ogren, L. Remer, T. Takemura, D. Tanre, O. Torres, C. R. Trepte, B. A. Wielicki, D. M. Winker, and H.
462 Yu (2005), A-Train strategy for quantifying direct climate forcing by anthropogenic aerosols, *Bull. Am. Meteorol.*
463 *Soc.*, **86(12)**, 1795-1809, doi: 10.1175/BAMS-86-12-1795

464 Angstrom, A. (1929), On the atmospherictr ansmission off Sun radiationa nd on dust in the air, Geogr. Ann., 12,
465 130-159.

466 Ansmann, A., H. Baars, M. Tesche, D. Muller, D. Althausen, R. Engelmann, T. Pauliquevis, and P. Artaxo (2009),
467 Dust and smoke transport from Africa to South America: Lidar profiling over Cape Verde and the Amazon
468 rainforest, Geophys. Res. Lett., 36, L11802, doi:10.1029/2009GL037923.

469 Bian, H, M. Chin, J. M. Rodriguez, H. Yu, J. E. Penner, and S. Strahan (2009), Sensitivity of aerosol optical
470 thickness and aerosol direct radiative effect to relative humidity. *Atmos. Chem. Phys.*, **9**, 2375–2386,
471 doi:10.5194/acp-9-2375-2009.

472 Bian, H., M. Chin, R. Kawa, H. Yu, T. Diehl, T. Kucsera (2010), Multi-scale aerosol and CO correlations from
473 MODIS and MOPITT satellites and GOCART model: implication for their emissions and atmospheric evolutions. *J.*
474 *Geophys. Res.*, Vol. 115, D077302, doi:10.1029/2009JD012781.

475 Cass, G. R., and F. H. Shair (1984), Sulfate accumulation in a sea breeze/land breeze circulation system, J. Geophys.
476 Res., 89, 1429-1438.

477 Delene, D. J., and J. A. Ogren (2002), Variability of aerosol optical properties at four North American surface
478 monitoing sites, *J. Atmos. Sci.*, **59(5315)**, 1135-1150, 2002. doi: 10.1175/1520-0469.

479 Doran, J. C. and S. Zhong (2000), Thermally driven gap winds in the Mexico City basin, *J. Appl. Meteorol.*, **39**,
480 1330–1340, doi: 10.1175/1520-0450

481 Eck, T. F., B. N. Holben, J. S. Reid, O. Dubovik, A. Smirnov, N. T. O'Neill, I. Slutsker, and S. Kinne (1999),
482 Wavelength dependence of the optical depth of biomass burning, urban, and desert dust aerosols, *J. Geophys. Res.*,
483 **104(D24)**, 31,333– 31,349, doi:10.1029/1999JD900923

484 Eck, T. F., B. N. Holben, D. E. Ward, M. M. Mukelabai, O. Dubovik, A. Smirnov, J. S. Schafer, N. C. Hsu, S. J.
485 Piketh, A. Queface, J. Le Roux, R. J. Swap, and I. Slutsker (2003), Variability of biomass burning aerosol optical
486 characteristics in southern Africa during the SAFARI 2000 dry season campaign and a comparison of single
487 scattering albedo estimates from radiometric measurements, *J. Geophys. Res.* , **108(D13)** , 8477,
488 doi:10.1029/2002JD002321.

489 Eck, T. F., B. N. Holben, O. Dubovik, A. Smirnov, P. Goloub, H. B. Chen, B. Chatenet, L. Gomes, X.-Y. Zhang, S.-
490 C. Tsay, Q. Ji, D. Giles, and I. Slutsker (2005), Columnar aerosol optical properties at AERONET sites in central

eastern Asia and aerosol transport to the tropical mid- Pacific, *J. Geophys. Res.*, **110**, D06202, 2005. doi:10.1029/2004JD005274.

Fast, J. D., B. de Foy, F. Acevedo Rosas, E. Caetano, G. Carmichael, L. Emmons, D. McKenna, M. Mena, W. Skamarock, X. Tie, R. L. Coulter, J. C. Barnard, C. Wiedinmyer, and S. Madronich (2007), A meteorological overview of the MILAGRO field campaigns, *Atmos. Chem. Phys.*, 7, 2233–2257, doi:10.5194/acp-7-2233-2007.

Fine, PM , B. Chakrabarti, M. Krudysz, JJ. Schauer, C. Sioutas (2004), Diurnal variations of individual organic compound constituents of ultrafine and accumulation mode particulate matter in the Los Angeles basin. *Environ. Sci. Technol.*, **38**, 1296-1304

Green, M. C., R. G. Flocchini, L. O. Myrup (1992). The relationship of the extinction coefficient distribution to wind field patterns in Southern California. *Atmos. Environ.*, **26A**, 827-840.

Holben, B. N, et al. (1998), AERONET — A federated instrument network and data archive for aerosol characterization, *Remote Sens. Environ.*, **66**, 1 –16, doi: 10.1016/S0034-4257(98)00031-5

Husar, R.B., J. M. Holloway, D. E. Patterson, and W. F. Wilson (1981), Spatial and temporal pattern of eastern U.S. haziness: A summary, Atmos. Environ., **15**, 1919-1928.

Kaufman, Y., B. N. Holben, D. Tanre, I. Slutsker, A. Smirnov, and T. F. Eck (2000), Will aerosol measurements from Terra and Aqua polar orbiting satellites represent the daily aerosol abundance and properties, *Geophys. Res. Lett.*, **27**, 3861-3864, 2000. doi:10.1029/2000GL011968

Lewis, E. R. and Schwartz S. E. (2004), Sea Salt Aerosol Production: Mechanisms, Methods, Measurements, and Models -- A Critical Review. *Geophysical Monograph Series* **Vol. 152**, American Geophysical Union, Washington.

Lu, R. and R. P. Turco (1994), Air pollutant transport in a coastal environment: Part I: Two-dimensional simulations of the sea-breeze and mountain effects. *J. atmos. Sci.* **51**, 2285-2308.

Lu, Rong and R. P. Turco (1995), Air pollutant transport in a coastal environment: Part II. Three-dimensional simulations over Los Angeles basin, *Atm. Environ.* **Vol. 29**, No. 13, pp. 1499-1518.

Malm, W. C. (1992), Characteristics and origins of haze in the continental Untied States, Earth-Science Reviews, **33**, 1-36.

Martin, S. T., et al. (2010), Sources and properties of Amazonian aerosol particles, Rev. Geophys., **48**, RG2002. doi:10.1029/2008RG000280.

Michalsky, J., F. Denn, C. Flynn, G. Hodges, P. Kiedron, A. Koontz, J. Schlemmer, and S. E. Schwartz (2010), Climatology of aerosol optical depth in north-central Oklahoma: 1992–2008, *J. Geophys. Res.*, **115**, D07203, doi:10.1029/2009JD012197.

Molina, L. T., C. E. Kolb, B. de Foy, B. K. Lamb, W. H. Brune, J. L. Jimenez, R. Ramos-Villegas, J. Sarmiento, V. H. Paramo-Figueroa, B. Cardenas, V. Gutierrez-Avedoy, and M. J. Molina (2007), Air quality in North America's most populous city – overview of the MCMA-2003 campaign, *Atmos. Chem. Phys.*, 7, 2447–2473. doi:10.5194/acp-7-2447-2007

National Research Council, Earth Science and Applications from Space: National Imperatives for the Next Decade and Beyond. *The National Academies Press*, Washington DC, 428pp (2007).

Pandithurai, G., R. T. Pinker, P. C. S. Devara, T. Takemura, and K. K. Dani (2007), Seasonal asymmetry in diurnal variation of aerosol optical characteristics over Pune, western India, *J. Geophys. Res.*, **112**, D08208, doi:10.1029/266JD007803.

Prados, A. I., S. Kondragunta, P. Ciren, and K. P. Knapp (2007), GOES Aerosol/Smoke Product (GASP) over North America: Comparisons to AERONET and MODIS observations, *J. Geophys. Res.*, **112**, D15201. doi:10.1029/266JD007968.

Prins, E. M., J. M. Feltz, W. P. Menzel, and D. E. Ward (1998), An overview of GOES-8 diurnal fire and smoke results for SCAR-B and 1995 fire season in South America, *J. Geophys. Res.*, **103(D24)**, 31,821–31,836. doi:10.1029/98JD01720

Raga, G. B., D. Baumgardner, G. Kok, and I. Rosas (1999), Some aspects of boundary layer evolution in Mexico City, *Atmos. Environ.*, **33(30)**, 5013–5021. doi: 10.1016/S1352-2310(99)00191-0

Reid, J. S., T. F. Eck, S. A. Christopher, P. V. Hobbs, and B. N. Holben (1999): Use of the Angstrom exponent to estimate the variability of optical and physical properties of aging smoke particles in Brazil, *J. Geophys. Res.*, **104**, 27 489–27 489.

Rissler, J., A. Vestin, E. Swietlicki, G. Fisch, J. Zhou, P. Artaxo, and M. O. Andreae (2006), Size distribution and hygroscopic properties of aerosol particles from dry-season biomass burning in Amazonia, *Atmos. Chem. Phys.*, **6**, 471–491. doi:10.5194/acp-6-471-2006

Salcedo, D., T. B. Onasch, K. Dzepina, M. R. Canagaratna, Q. Zhang, J. A. Huffman, P. F. DeCarlo, J. T. Jayne, P. Mortimer, D. R. Worsnop, C. E. Kolb, K. S. Johnson, B. Zuberi, L. C. Marr, R. Volkamer, L. T. Molina, M. J. Molina, B. Cardenas, R. M. Bernab´e, C. M´arquez, J. S. Gaffney, N. A. Marley, A. Laskin, V. Shutthanandan, Y. Xie, W. Brune, R. Lesher, T. Shirley, and J. L. Jimenez (2006), Characterization of ambient aerosols in Mexico City during the MCMA-2003 campaign with Aerosol Mass Spectrometry: results from the CENICA Supersite, *Atmos. Chem. Phys.*, **6**, 925–946. doi:10.5194/acp-6-925-2006

Schafer, J. S., T. F. Eck, B. N. Holben, P. Artaxo, and A. F. Duarte (2008), Characterization of the optical properties of atmospheric aerosols in Amazo^nia from long-term AERONET monitoring (1993–1995 and 1999–2006), *J. Geophys. Res.*, **113**, D04204,. doi:10.1029/2007JD009319

Seinfeld, J. H., and S. N. Pandis, Atmospheric chemistry and physics, Chapter 9. 1998, *Wiley-Interscience publication*

Smirnov, A., B. N. Holben, T. F. Eck, O. Dubovik, and I. Slutsker (2000), Cloud screening and quality control algorithms for the AERONET data base, *Remote Sens. Environ.*, **73**, 337–349, **DOI:** 10.1016/S0034-4257(00)00109-7

Smirnov, A., B. N. Holben, T. F. Eck, I. Slutsker, B. Chatenet, and R. T. Pinker (2002), Diurnal variability of aerosol optical depth observed at AERONET (Aerosol Robotic Network) sites, *Geophys. Res. Lett.*, **29**, 2115, doi:10.1029/2002GL016305.

Smirnov, A., B. N. Holben, O. Dubovik, R. Frouin, T. F. Eck, and I. Slutsker (2003), Maritime component in aerosol optical models derived from Aerosol Robotic Network data, *J. Geophys. Res.*, **108(D1)**, 4033, doi:10.1029/2002JD002701.

Sun, Y.L., et al. (2011), A case study of aerosol processing and evolution in summer in New York City, Atmos. *Phys. Chem. Disccuss.*, **11**, 25751-25784.

570 Wakimoto, R. M., and J. L. McElroy (1986), Lidar observation oof elevated pollution layers oover Los Angeles, *J.*
571 *Clim. Appl. Meteorol.*, **25**, 1583-1599.

572 Wang, J., U. S. Nair, and S. A. Christopher (2004), GOES 8 aerosol optical thickness assimilation in a mesoscale
573 model: Online integration of aerosol radiative effects, *J. Geophys. Res.*, **109**, D23203. doi:10.1029/2004JD004827.
574
575 Whiteman, C. D., S. Zhong, X. Bian, J. D. Fast, and J. C. Doran (2000), Boundary layer evolution and regional-scale
576 diurnal circulations over the Mexican basin, *J. Geophys. Res.*, **105(D8)**, 10 081–10 102, doi:10.1029/2000JD900039

577 Yu, H., S. C. Liu, and R. E. Dickinson (2002), Radiative effects of aerosols on the evolution of the atmospheric
578 boundary layer, *J. Geophys. Res.*, **107(D12)**, 4142. doi:10.1029/2001JD000754

579 Yu, H., R. E. Dickinson, M. Chin, Y. Kaufman, M. Zhou, L. Zhou, Y. Tian, O. Dubovik, and B. Holben (2004),
580 Direct radiative effect of aerosols as determined from a combination of MODIS retrievals and GOCART simulations,
581 *J. Geophys. Res.*, **109**, D03206. doi:10.1029/2003JD003914

582 Yu H., M. Chin, D. M. Winker, A. H. Omar, Z. Liu, C. Kittaka, and T. Diehl (2010). Global view of aerosol vertical
583 distributions from CALIPSO lidar measurements and GOCART simulations: Regional and seasonal variations, *J.*
584 *Geophys. Res.*, **115**, D00H30 doi:10.1029/2009JD013364

585
586

587

Figure 1. Geographical distributions of seasonal mean aerosol optical depth (AOD) at 440 nm (aggregated into 5 bins and marked with different colors), AOD daytime variation range (DVR is defined as a difference of maximum and minimum hourly percentage departure from the daily mean AOD, with its value being represented by size of triangle), and occurring time of maximum AOD (with upside triangle for morning and downside triangle for afternoon).

Figure 2. Same as Figure 1 but for aerosol Angstrom exponent (AE) (over 440-870 nm)

Figure 3. Percentage deviations of hourly average aerosol optical depth (AOD at 440 nm) relative to the daily mean in all seasons for sites over Mid-Atlantic U.S. The map in the right-down corner in MAM shows location of sites. The vertical bar represents the standard error of measurements in each hour. Seasonal mean AOD for each sites are also shown in the figure.

Figure 4. Diurnal Relative humidity profiles from GEOS-4 at 10, 13 and 16 local standard time over mid-Atlantic sites in 2007.

Figure 5. Same as Figure 3 but for four sites in U.S. West coast.

Figure 6: Percentage deviations of hourly average aerosol optical depth (AOD at 440 nm, using left y-axis) and Angstrom exponent (AE over 440-870 nm range, using right y-axis) relative to the daily mean in four seasons in Mexico City. The vertical bar represents the standard error of measurements in each hour. Seasonal mean AOD and AE are also shown in the figure.

Figure 7: same as Figure 3 but for sites over Amazon region during the dry season (Aug-Oct, ASO)

Figure 8. Percentage deviations of hourly average aerosol optical depth (AOD at 440 nm) relative to the daily mean for August, September, and October at Alta Floresta and Cuiaba-Miranda.

Figure 9. Same as Figure 5 but for Lanai.

620 Figure 10. Deviations of hourly average aerosol optical depth (AOD at 440 nm) in four seasons
621 at Table Mountain.

622

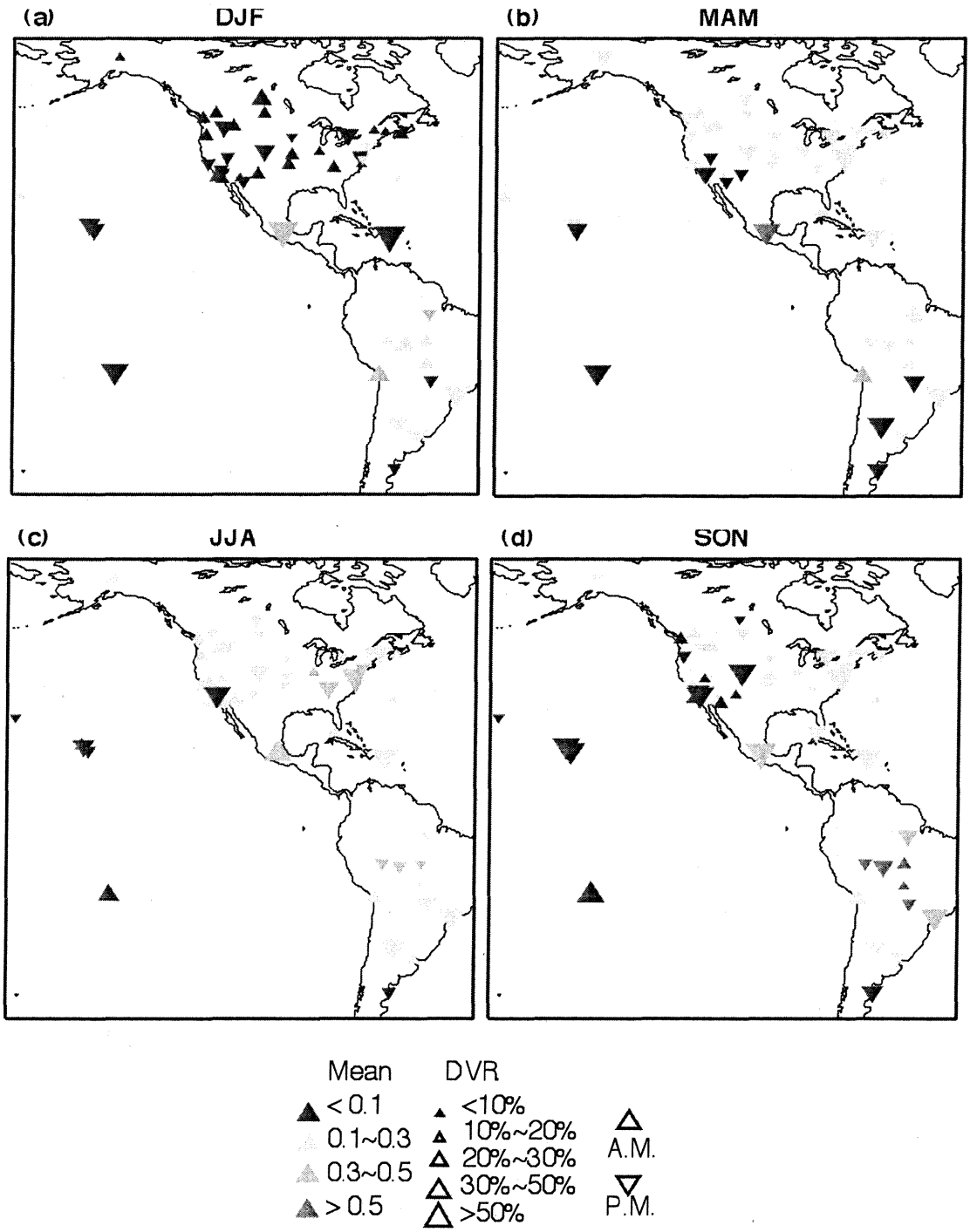

Figure 1. Geographical distributions of seasonal mean aerosol optical depth (AOD) at 440 nm (aggregated into 5 bins and marked with different colors), AOD daytime variation range (DVR is defined as a difference of maximum and minimum hourly percentage departure from the daily mean AOD, with its value being represented by size of triangle), and occurring time of maximum AOD (with upside triangle for morning and downside triangle for afternoon).

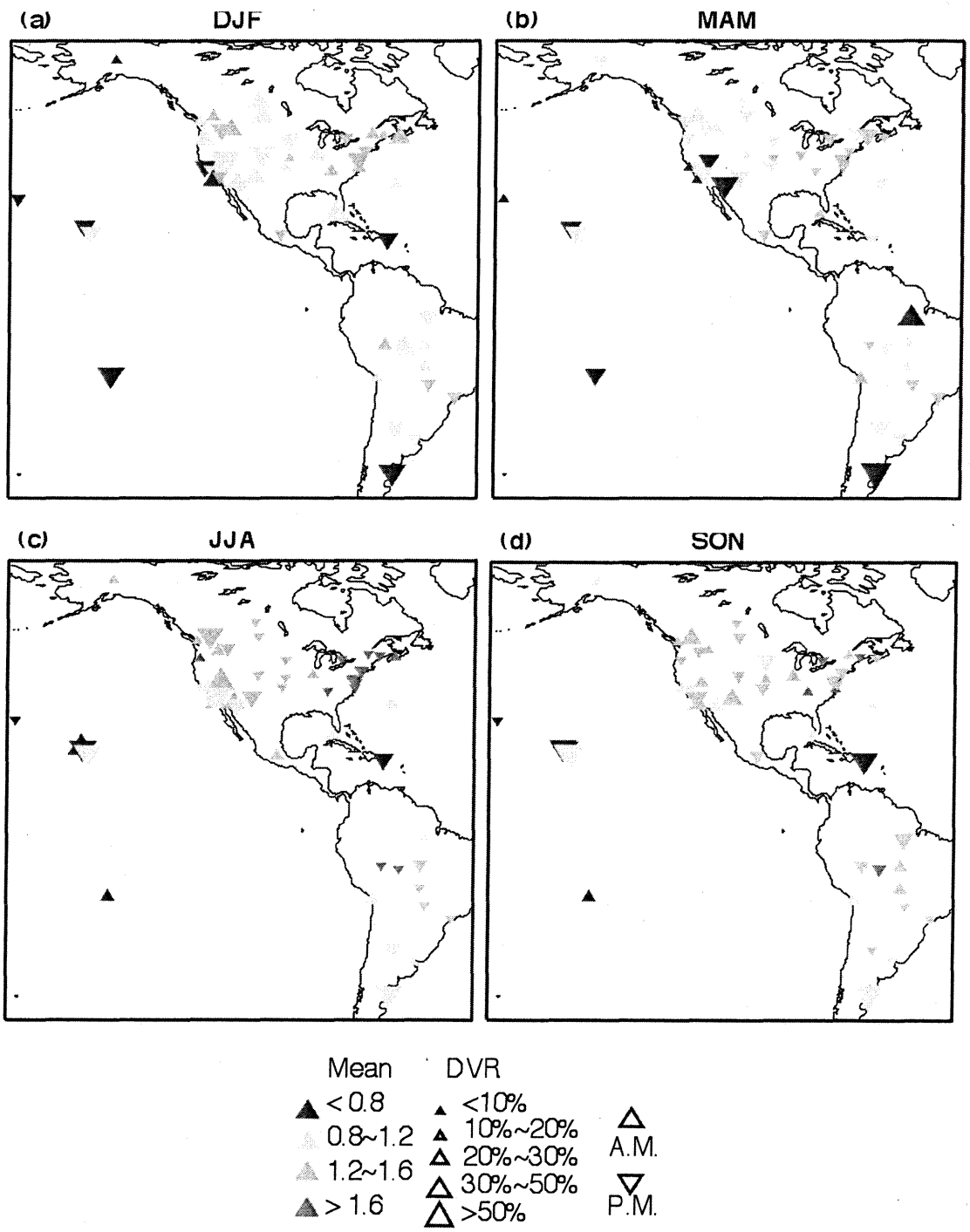

Figure 2. Same as Figure 1 but for aerosol Angstrom exponent (AE) (over 440-870 nm).

637

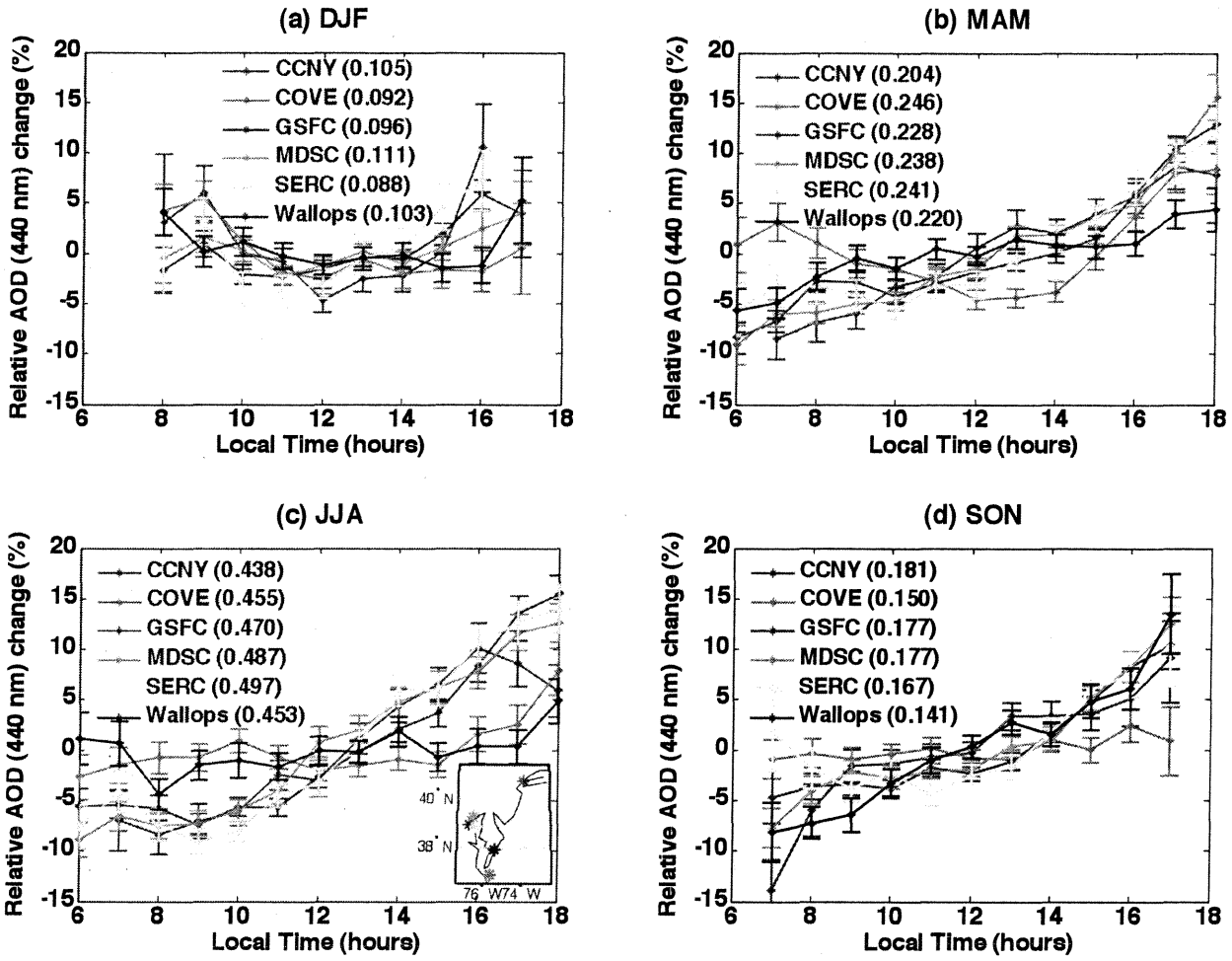

638

639

640 Figure 3. Percentage deviations of hourly average aerosol optical depth (AOD at 440 nm)
641 relative to the daily mean in all seasons for sites over Mid-Atlantic U.S. The map in the right-
642 down corner in MAM shows location of sites. The vertical bar represents the standard error of
643 measurements in each hour. Seasonal mean AOD for each sites are also shown in the figure.

644

645

646

647

ERROR: limitcheck
OFFENDING COMMAND: image

Figure 4

Figure 4. Diurnal Relative humidity profiles from GEOS-4 at 10, 13 and 16 local standard time over mid-Atlantic sites in 2007.